Journal of *Marine Science and Engineering*

MDPI

*Article*

# Detection of Seismic and Acoustic Sources Using Distributed Acoustic Sensing Technology in the Gulf of Catania

**Abdelghani Idrissi [1,*], Danilo Bonanno [1], Letizia S. Di Mauro [1], Dídac Diego-Tortosa [1], Clara Gómez-García [2], Stephan Ker [3], Florian Le Pape [3], Shane Murphy [3], Sara Pulvirenti [1], Giorgio Riccobene [1], Simone Sanfilippo [1] and Salvatore Viola [1]**

[1] Laboratori Nazionali del Sud (LNS)—Istituto Nazionale di Fisica Nucleare (INFN), Via S. Sofia 62, 95125 Catania, Italy
[2] Centro Siciliano di Fisica Nucleare e Struttura della Materia (CSFNSM), Via S. Sofia 64, 95123 Catania, Italy
[3] Geo-Ocean, Institut Français de Recherche pour l'Exploitation de la Mer (IFREMER)—Centre National de la Recherche Scientifique (CNRS), UMR6538 University Brest, 1625 Rte de Sainte-Anne, 29280 Plouzané, France
* Correspondence: abdelghani.idrissi@lns.infn.it; Tel.: +39-095542111

**Abstract:** Distributed Acoustic Sensing (DAS) technology presents an innovative method for marine monitoring by adapting existing underwater optical fiber networks. This paper examines the use of DAS with the Istituto Nazionale di Fisica Nucleare–Laboratori Nazionali del Sud (INFN-LNS) optical fiber infrastructure in the Gulf of Catania, Eastern Sicily, Italy. This region in the Western Ionian Sea provides a unique natural laboratory due to its tectonic and volcanic activity, proximity to Mount Etna, diverse marine ecosystems and significant human influence through maritime traffic. By connecting a 28 km long optical cable to an Alcatel Submarine Network OptoDAS interrogator, DAS successfully detected a range of natural and human–made signals, including a magnitude 3.5 ML earthquake recorded on 14 November 2023, and acoustic signatures from vessel noise. The earthquake–induced Power Spectral Density (PSD) increased to up to 30 dB above background levels in the 1–15 Hz frequency range, while vessel noise exhibited PSD peaks between 30 and 60 Hz with increases of up to 5 dB. These observations offered a detailed spatial and temporal resolution for monitoring seismic wave propagation and vessel acoustic noise. The results underscore DAS's capability as a robust tool for the continuous monitoring of the rich underwater environments in the Gulf of Catania.

**Keywords:** distributed acoustic sensing; shipping noise; underwater acoustics



Academic Editor: Manuel Martín-Martín

Received: 30 January 2025
Revised: 27 February 2025
Accepted: 21 March 2025
Published: 25 March 2025

**Citation:** Idrissi, A.; Bonanno, D.; Di Mauro, L.S.; Diego-Tortosa, D.; Gómez-García, C.; Ker, S.; Le Pape, F.; Murphy, S.; Pulvirenti, S.; Riccobene, G.; et al. Detection of Seismic and Acoustic Sources Using Distributed Acoustic Sensing Technology in the Gulf of Catania . *J. Mar. Sci. Eng.* **2025**, *13*, 658. https://doi.org/10.3390/jmse13040658



## 1. Introduction

Distributed Acoustic Sensing (DAS) technology uses optical fibers as sensors to detect and measure acoustic and seismic vibrations along their entire length. Unlike traditional sensors, which gather data at discrete points, DAS systems provide continuous, high-resolution measurements, especially in areas where traditional sensors face a lot of challenges [1]. This capability for spatially distributed measurements allows the near-real-time monitoring of extensive environments. A DAS system operates by transmitting short, coherent pulses of laser light into an optical fiber, where the light interacts with microscopic imperfections in the glass, producing backscattered light. This backscattered light, primarily consisting of Rayleigh scattering, is sensitive to external influences such as vibrations, strain or acoustic waves. These disturbances cause changes in the phase, frequency and intensity of the backscattered light. By processing these variations using advanced signal

analysis techniques, typically involving optical interferometry, DAS systems can precisely determine the location and nature of a disturbance [2].

In the last decade, DAS technology has become widely adopted across multiple fields due to its versatility. In pipeline monitoring, DAS can detect leaks, ground movement and unauthorized digging, providing early warning of catastrophic failures [3,4]. In civil engineering, it is currently considered one of the most innovative methodologies for monitoring structural health and strain and stress levels, especially in major infrastructure such as bridges, tunnels or dams [5]. Additionally, DAS enhances perimeter security by providing near-real-time detection of intrusions or unusual activities along extended boundaries [6,7]. In geophysics, DAS enhances spatial resolution for seismic monitoring, capturing both local and regional events. It also tracks wave propagation over the entire length of the fiber–optic cable with high spatial resolution, proving DAS to be a useful addition to early warning systems for earthquakes, volcanic eruptions and other geophysical hazards [8,9]. Recently, researchers have started exploring the potential of DAS for estimating earthquake magnitudes and localizing seismic events [10–12]. DAS is a promising tool for complementing traditional deployments of seismometer arrays, many of which are seriously limited in their coverage, especially over areas where deploying traditional seismic sensors is difficult, like the Arctic and Antarctic regions, volcanoes or deep ocean seafloors [13].

DAS has proven to be a powerful tool for seabed monitoring in marine environments [14,15], particularly in the offshore oil and gas sector, where accurate seismic data are important for both exploration and safety. Beyond its role in resource industries, DAS is increasingly used to monitor seismic activities, underwater events such as submarine landslides and anthropogenic activities such as shipping traffic [16]. Fiber–optic cables deployed along coastlines or on the ocean floor also offer the potential to monitor tsunami waves and storms in real time [17,18]. DAS's ability to cover extensive areas with high sensitivity, all without the need for extra seabed sensors, makes it a powerful monitoring tool in challenging environments like the deep sea [19,20]. However, deploying DAS in marine environments, especially on the seabed, poses significant technical and logistical challenges due to harsh underwater conditions like extreme pressure, corrosive saltwater and limited accessibility for maintenance. Installing new fiber optics is both complex and costly, requiring meticulous planning and significant resources. Ensuring long–term reliability is of primary importance, as cable failures could lead to data loss or necessitate expensive repairs. To address these challenges, repurposing existing underwater fiber networks, originally deployed for telecommunications or scientific research, offers a cost–effective solution. However, using previously deployed cables for deep–sea DAS experiments can present challenges [21]. The way the cable interacts with the seabed, whether it is tightly coupled, partially buried or suspended in the water column, can influence its sensitivity to acoustic and seismic signals by affecting how external vibrations are transferred to the fiber. Additionally, if the cable contains connectors, they can introduce signal attenuation due to losses and reflections, which, in turn, limit sensitivity over long distances.

The purpose of this work is to demonstrate the potential of DAS technology for marine environment seismic and acoustic detection. To achieve this, we used an Alcatel Submarine Network OptoDAS interrogator unit to interrogate an existing underwater optical fiber network originally installed for deep–sea scientific research and neutrino detection as part of the NEMO (NEutrino Mediterranean Observatory) project [22]. By leveraging the Istituto Nazionale di Fisica Nucleare–Laboratori Nazionali del Sud (INFN–LNS) seabed infrastructure located in the Gulf of Catania [23], Eastern Sicily, we address the challenges of marine monitoring innovatively. This region in the Western Ionian Sea, off the eastern coast of Sicily, was chosen for this study due to its exceptional combination of geophysical,

biological and anthropogenic features. It is one of the most seismically active areas in the Mediterranean, located near the converging African and Eurasian tectonic plates. Some of the most outstanding geophysical features in this region include Mount Etna, Europe's most active volcano [24], which significantly impacts the area's seismicity [25]. Additionally, the Western Ionian Sea has intense maritime activity, leading to substantial vessel traffic [26]. The region is also recognized for its abundant marine biodiversity, particularly the presence of marine mammals, offering tremendous value for biological research and conservation efforts [27,28]. The interplay of active seismic zones, heavy maritime traffic and rich marine ecosystems creates a distinctive environment for acoustic studies, positioning the Ionian Sea as an ideal site for deploying DAS technology to monitor both natural and anthropogenic underwater acoustic signals.

## 2. Materials and Methods

### 2.1. INFN–LNS Deep–Sea Optical Fiber Infrastructures

The INFN–LNS operates an advanced deep–sea cabled infrastructure off the eastern coast of Sicily, in the Gulf of Catania, as shown in Figure 1. This infrastructure connects a shore laboratory located in the Port of Catania to two underwater sites in the Gulf of Catania through a 28 km electro–optical submarine cable with 10 optical fibers. The cable is Y–junctioned 25 km offshore, leading to two separate cable termination frames, TSN (Test Site North) and TSS (Test Site South), positioned at approximately 2100 m water depth. This infrastructure provides significant support to a variety of Italian and European scientific research projects such as Geoinquire, EMSO–ERIC [29], IPANEMA/ECCSEL–ERIC [30] and FOCUS–ERC [31]. In particular, within the ERC projects FOCUS–ERC and Geoinquire, cutting–edge DAS and BOTDR (Brillouin Optical Time–Domain Reflectometry) technologies have been installed for deep–sea long–term monitoring. This extensive optical network, coupled with its advanced sensing technologies, provides unprecedented opportunities for scientific research and advancing our understanding of deep–sea ecosystems and their interactions [23].

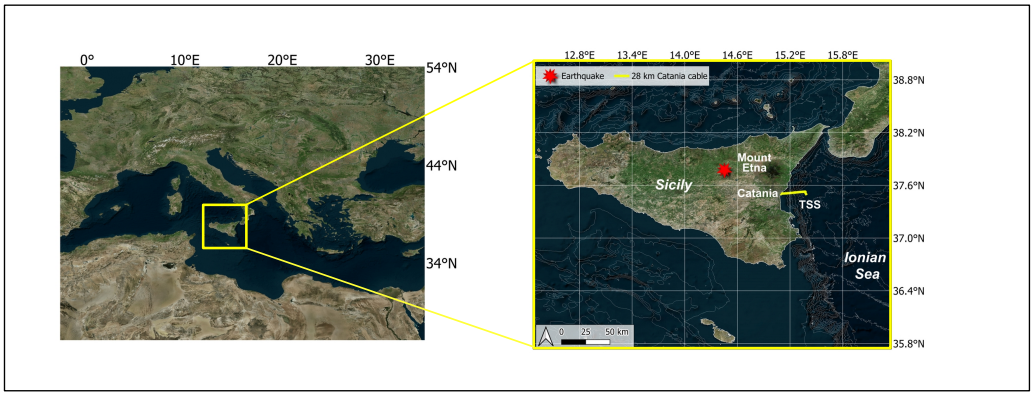


**Figure 1.** Map showing the location of the INFN–LNS deep–sea cabled infrastructure off the coast of Eastern Sicily. The map also highlights the location of Mount Etna and an earthquake event captured during the experiment on 14 November 2023.

### 2.2. Experimental Setup

To assess the capabilities of the INFN–LNS infrastructures for monitoring both natural and anthropogenic signals using DAS, a series of measurements was conducted between 9 and 16 November 2023. During this campaign, IFREMER utilized an Alcatel Submarine Network (ASN) OptoDAS to interrogate two seafloor electro–optical cables within the INFN–LNS marine infrastructure in Eastern Sicily. The DAS system was connected to the LNS–INFN electro–optical cable, which extends 28 km from the Port of Catania to

its termination at approximately 2100 m water depth. This cable is characterized by an optical attenuation of 0.25 dB/km at a laser wavelength of 1550 nm. The system operates by measuring the phase difference between two points along the fiber, which are separated by a distance equal to the gauge length, an approach based on the optical time–domain reflectometry (OTDR) technique [32]. By analyzing the phase shifts in the backscattered light over time, the system detects small variations in the optical path length caused by external acoustic or mechanical disturbances. These phase variations can then be transformed into strain measurements [33]. During the measurements, the interrogator was configured with a sampling frequency of 250 Hz, a channel spacing of approximately 2 m and a gauge length of 10.2 m. Since the channel spacing between consecutive measurement points along the fiber was smaller than the gauge length, each gauge length overlapped with the next. Additionally, for accurate time stamping and synchronization, a Global Positioning System (GPS) receiver was used to provide precise timing references. To ensure stable operation, the laser source required a warm–up period of 1–2 h before data acquisition. Data and their associated metadata were stored in HDF5 (Hierarchical Data Format version 5) file format, which ensures efficient organization and accessibility for large datasets. Each 10-s file contained 2500 time samples, resulting in a file size of more than 200 MB. These configurations yielded an effective spatial resolution over the length of the cable.

## 3. Results and Discussion

### *3.1. Seismic Event Detection*

On 14 November 2023, an earthquake was recorded along the Catania cable using the DAS system. Figure 2a shows a time–distance representation of the seismic wave arrivals, with the faster Primary (P) waves followed by the slower Secondary (S) waves. The earthquake, with a magnitude of ML 3.5, occurred at 14:04:52 UTC near Nicosia, Italy, at a depth of 28 km and at geographic coordinates (37.7730, 14.4530) [34]. Recently, researchers have begun exploring the potential of using DAS for estimating earthquake magnitude. Yin et al. (2023) [10] took a step in this direction by developing the first scaling relationship between DAS peak amplitude and earthquake magnitude. The seismic waves were detected on the cable at 14:05:04 UTC, approximately 12 s after the event. Based on the measured propagation distance of 64 km from the epicenter to the cable, the velocity of the P–waves can be estimated as approximately 5.33 km/s. This value aligns with the expected velocities for P–waves traveling through the Earth's crust at similar depths [35]. The frequency content of the seismic signal is displayed in the spectrogram shown in Figure 2b, computed using a 1024–point FFT with 98% overlap. The spectrogram reveals a dominant low–frequency energy component, predominantly below 20 Hz, characteristic of earthquake–generated seismic waves. These results underscore the capability of DAS to deliver detailed temporal, spatial and spectral information during seismic events. The unprecedented level of information on wave arrivals and propagation dynamics highlights the capability of DAS to effectively complement traditional seismic monitoring networks.

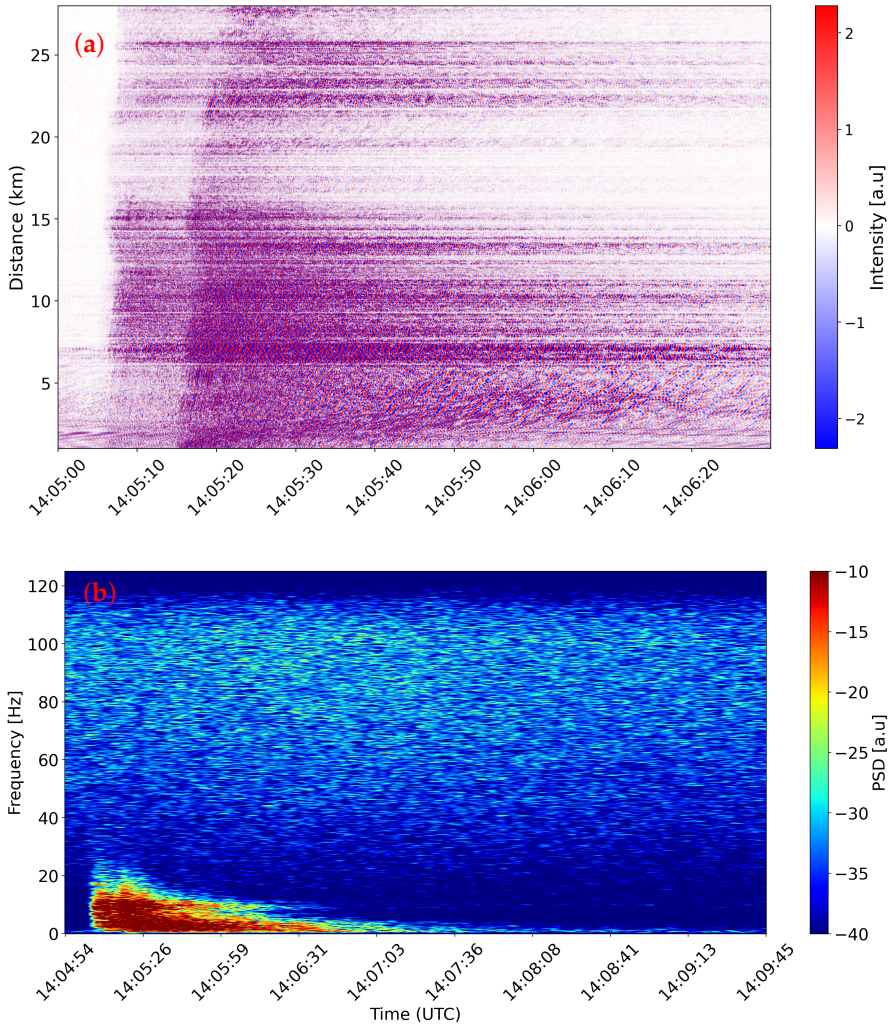


**Figure 2.** Earthquake event recorded on 14 November 2023. (**a**) Time–distance representation of the signal after applying a 25 Hz low–pass filter, where the *x*–axis represents time in UTC, the *y*–axis shows the distance along the cable and the color scale indicates the amplitude of the signal. (**b**) Spectrogram derived using 5 min data, displaying frequency content over time. The spectrogram was computed using a 1024–point FFT with a 98% overlap based on the method described in [36]. The analysis was based on data from a single channel located at a distance of approximately 12 km from the interrogator.

In Figure 2a, a reduction in the signal amplitude can be observed between 16 and 21 km from shore. This pattern also appears during background noise recordings, mainly at low frequencies, as represented in Figure 3, suggesting that it is not caused by the seismic event itself but is likely related to the cable or its environment. For example, variations in the cable's coupling to the seabed, such as suspension, burial or poor mechanical contact, could result in distorted sensitivity in this segment [20,37]. Additionally, intrinsic optical losses in the cable, such as attenuation due to microbending or stress, or environmental factors like localized changes in sediment composition or seabed structure, may play a role. This variation in the signal amplitude emphasizes the importance of taking the cable's condition and the local environment into account when interpreting DAS data. It also indicates the necessity for further research to better understand and optimize the system's performance.

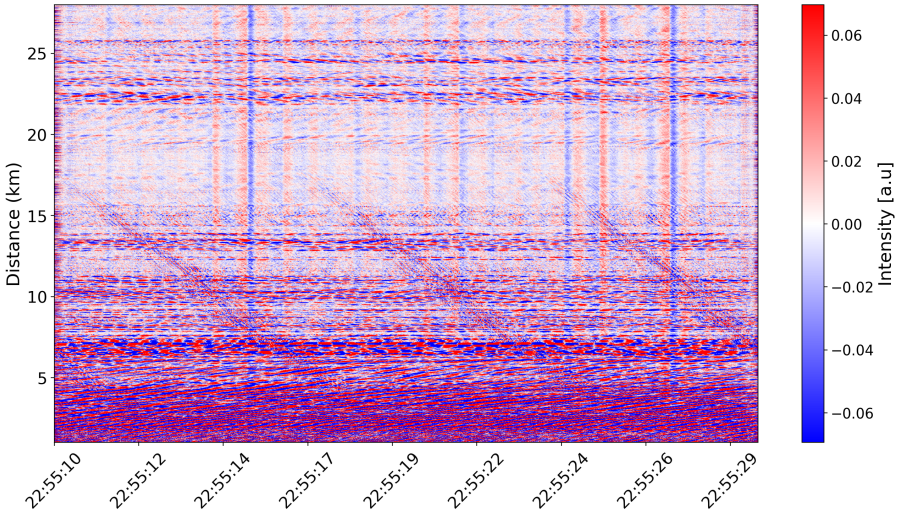


**Figure 3.** Twenty–seconds time–distance plot of the background noise recording after applying a 1–10 Hz pass–band filter.

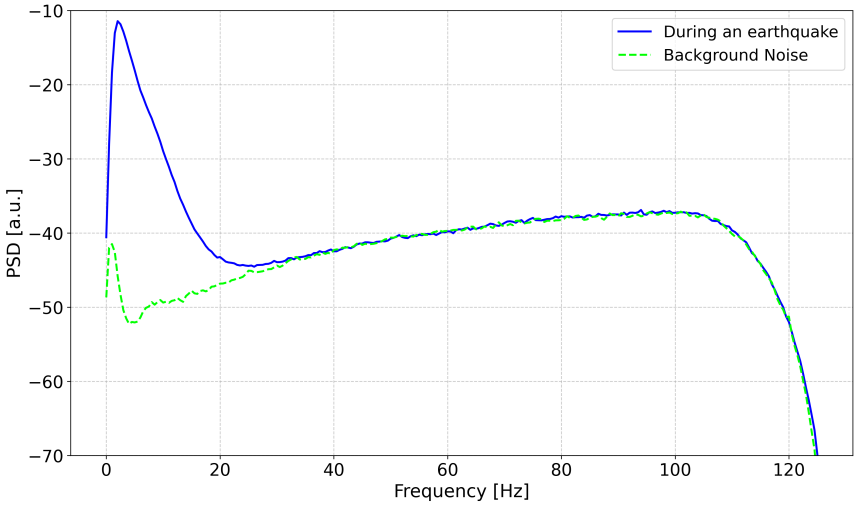


**Figure 4.** Comparison of PSD during an earthquake and the ambient noise. The result was obtained using 40 s of DAS data and averaged over a 10 km cable section between 5 km and 15 km.

Figure 4 shows a Power Spectral Density (PSD) comparison between an earthquake event and the common background noise, revealing a broader spectral energy distribution, particularly concentrated in the low–frequency range below 20 Hz. The earthquake–induced PSD exhibits an increase to up to about 30 dB above background noise levels, with energy spikes notably present between 1 and 15 Hz. This pronounced low–frequency component is a defining characteristic of seismic activity, distinguishing it from anthropogenic noise sources such as vessel traffic, which typically exhibit harmonic peaks at higher frequencies, as shown in Figure 5. The energy gradually declines beyond 20 Hz and aligns with background noise above 30 Hz. Furthermore, in the PSD of the background noise, a small peak appears at frequencies below 3 Hz. This increase in energy comes mainly from teleseismic events, microseisms and ocean waves. In Figure 6, we present a PSD comparison along different cable sections. This plot shows a noticeable increase in energy levels in the shallow–water section (1–6 km) compared to the deeper sections. This increase in low–frequency energy is always present in the first 5 km section of the optical fiber, as shown in Figure 3. This increase in signal amplitude is mainly due to the surface gravity waves. In the deeper sections, the energy levels are lower because gravity–wave–induced seabed motion decays with depth. As the water depth increases,

the seabed is less affected by surface gravity waves, leading to reduced low–frequency noise [38].

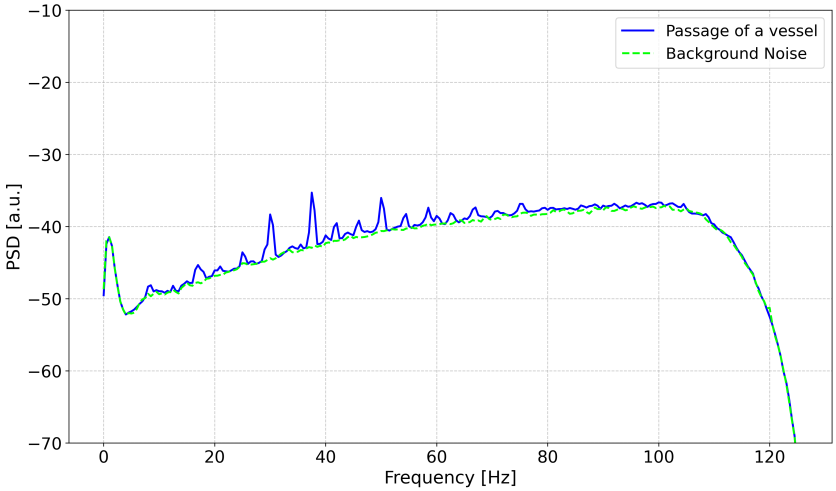


**Figure 5.** Comparison of PSD during the passage of a vessel and the ambient noise. Results were obtained using 40 s of DAS data and averaged over a 10 km cable section between 5 km and 15 km focusing on the closest section to the vessel's track.

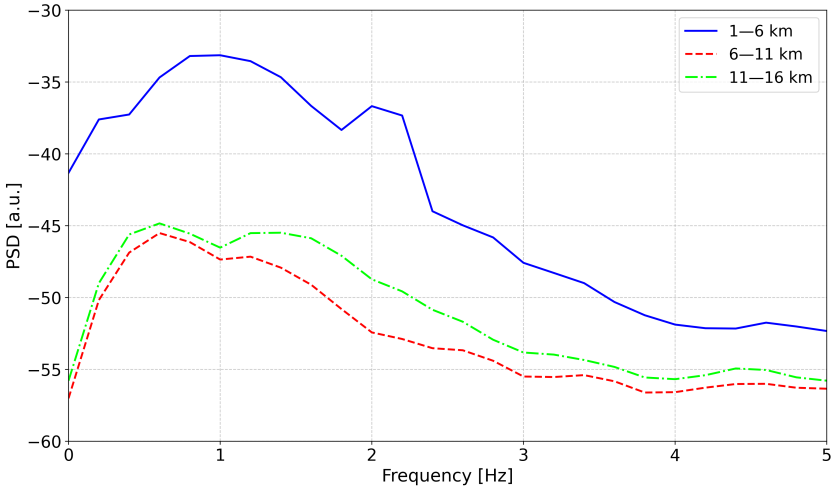


**Figure 6.** Comparison of PSD of background noise along different sections of the cable with a focus on low frequencies (0–5 Hz).

### *3.2. Anthropogenic Signals: Shipping Traffic Monitoring*

In addition to natural seismic events, the DAS system also recorded anthropogenic signals, particularly vessel noise. Figure 7 shows an example of a vessel that crossed on top of the optical fiber on 15 November 2023, at a distance of about 12 km from the shore (from the interrogator). At this distance, the optical fiber is laid at a water depth of more than 800 m. In Figure 7a, the vessel sound signature can be observed clearly along a more than 5 km long cable section. The observed hyperbolic or V–shape of the wavefront arises from time–of–arrival delay, where the acoustic signal reaches different sections (channels) of the fiber at slightly different times. This pattern indicates the vessel's bearing and motion relative to the cable. However, DAS's symmetrical strain response introduces a left–right ambiguity (or 180° ambiguity) [18]. To address this limitation, the integration of hydrophone arrays, an Automatic Identification System (AIS) and strategic cable geometries present effective remedies for this ambiguity. An array of three or more hydrophones resolves the left–right ambiguity of the DAS system by taking advantage of

time–of–arrival differences to distinguish signals originating from either side of the cable. Additionally, deploying fibers in specific geometric configurations such as loops, curves or bends introduces asymmetry in the strain response along the cable, naturally resolving directional ambiguities as strain patterns vary with the vessel's position relative to the cable geometry.

Figure 5 represents a PSD comparison of the passage of a vessel close to the cable and the common background noise. The PSD associated with the vessel's noise shows multiple pronounced peaks between 10 and 80 Hz, as depicted also in the spectrogram in Figure 7b, a common signature of shipping noise. These peaks likely correspond to the propeller blade rate and harmonics generated by vessel engines and mechanical systems. The most significant peaks occur in the lower–frequency range (30–60 Hz), where noise levels increased to up to 5 dB above the background noise, which is typical for the low–frequency noise produced by large vessels [16]. In addition, an increase in the noise level can be observed in Figure 7b, mainly in the frequency range of 70–110 Hz. This behavior could be explained by the noise generated by the formation, growth and collapse of vapor bubbles in a liquid due to rapid changes in pressure, which is known in the literature as cavitation noise [39,40].

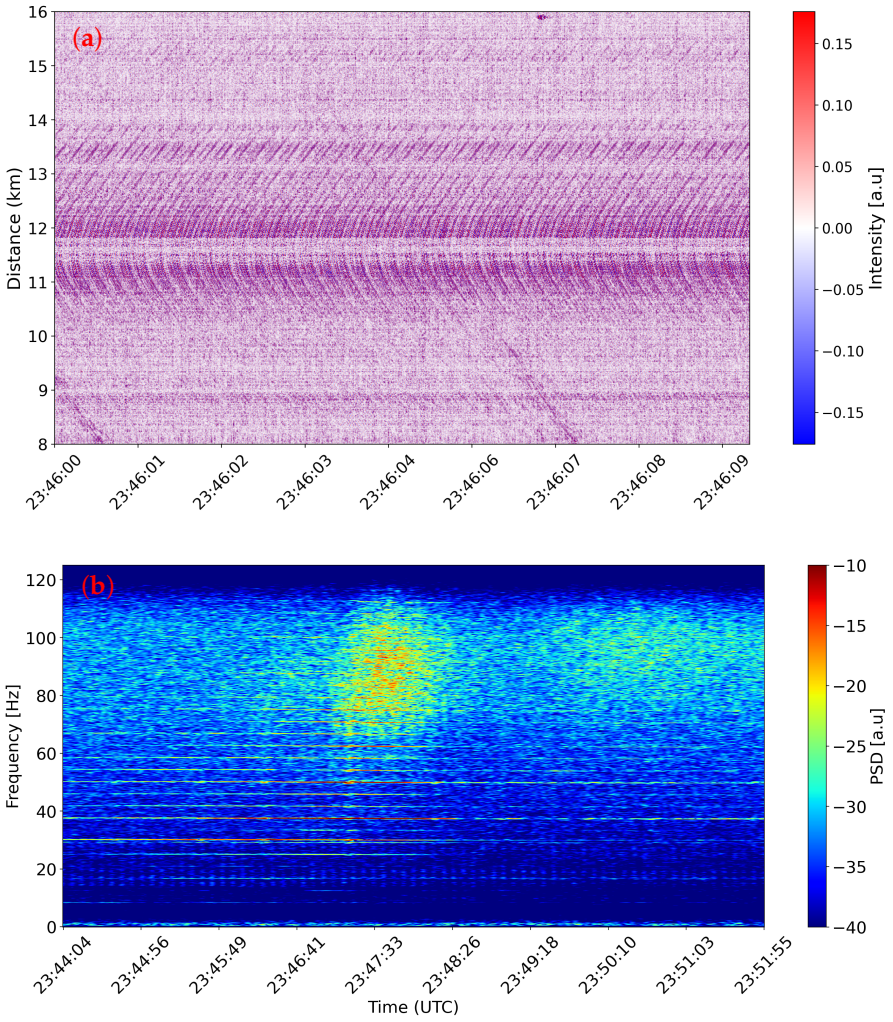


**Figure 7.** Vessel signal recorded on 15 November 2023. (**a**) Ten–seconds time–distance representation of the signal after applying a 35–124 Hz pass–band filter, where the $x$–axis represents time in UTC, the $y$–axis shows the distance along the 28 km cable length and the color scale represents the signal amplitude. (**b**) Spectrogram derived from 8 min recording using channel data at a distance of 12 km from the interrogator computed using a 1024–point FFT with 98% overlap.

Additionally, the third–octave band centered at 63 Hz (covering the frequency range from approximately 56.2 Hz to 70.8 Hz), which is one of the primary frequency bands monitored under the Marine Strategy Framework Directive (MSFD) [41,42] to assess continuous low–frequency shipping noise pollution, exhibits a noticeable increase in energy levels during the vessel's passage. This reinforces the relevance of monitoring ship–generated noise, as prolonged exposure to elevated levels in this frequency range has been shown to impact marine species that rely on low–frequency communication [43]. The ability of DAS technology to detect these spectral variations in real time provides a scalable and cost–effective solution for the long–term monitoring of anthropogenic noise in marine environments. This not only helps in enforcing MSFD Descriptor 11 regulations but also contributes to broader environmental conservation efforts by providing data to mitigate the effects of human activities on marine ecosystems.

## 4. Conclusions and Perspectives

By deploying DAS technology on the INFN–LNS deep–sea infrastructure in the Gulf of Catania, this study demonstrates its potential for monitoring deep–sea environments. Utilizing a 28 km long optical fiber, the DAS system successfully detected a wide range of signals, including a seismic event and shipping noise. The seismic waves were observed along the entire length of the optical fiber, with dominant energy at low frequencies of below 20 Hz. On the other hand, vessel acoustic signatures were only recorded along a portion of the cable (around an 8 km section), with frequency peaks in the range of 10 to 80 Hz. The PSD analysis also revealed distinct characteristics for each event. The earthquake showed an increase to up to 30 dB above background levels, whereas vessel noise only rose by as much as 5 dB.

These results highlight DAS as a valuable tool for the passive, continuous monitoring of both natural and human activities, with applications across geophysics, applied physics and marine biology. Its use of existing fiber–optic infrastructures makes it an environmentally friendly approach, while studies of vessel traffic could help mitigate noise pollution affecting cetaceans. This multidisciplinary potential strengthens the case for integrating DAS with complementary technologies, such as hydrophone arrays, to enhance marine monitoring efforts.

Recently, INFN–LNS started operating a new deep–sea cabled observatory as part of the IPANEMA project [30]. This station is equipped with four synchronized hydrophones installed at a depth of over 2000 m connected to the TSS point at the end of the 28 km long electro–optical cable, which is the same infrastructure used in the presented DAS experiment. This hydrophone array not only enhances acoustic source localization, providing precise tracking of vessel acoustic signatures and marine life such as fin whale migrations, but also offers an excellent opportunity to complement DAS technology. Furthermore, the hydrophone data can be used to calibrate DAS recordings [44], or at least some channels of the system. Future experiments aim to explore and enhance the integration of DAS and hydrophone arrays to expand their capabilities and improve monitoring accuracy.

**Author Contributions:** Methodology, A.I., L.S.D.M., D.D.-T., C.G.-G., S.K., F.L.P., S.M., S.P., G.R., S.S. and S.V.; Software, A.I., S.S. and S.V.; Validation, G.R.; Formal analysis, A.I., D.D.-T. and C.G.-G.; Investigation, A.I., L.S.D.M., D.D.-T. and S.P.; Resources, S.K., F.L.P. and S.M.; Writing—original draft, A.I.; Writing—review & editing, D.D.-T. and C.G.-G.; Supervision, D.B., G.R. and S.V. All authors have read and agreed to the published version of this manuscript.

**Funding:** This research received no external funding.

**Institutional Review Board Statement:** Not applicable.

**Data Availability Statement:** Contact the corresponding author to request data or information about it.

**Acknowledgments:** The support of the INFN Experimental Fellowship through the Post–Doctoral Senior Level 3 Research Grant B.C. no. 23591/2021, which funded Diego–Tortosa as a postdoctoral researcher, is gratefully acknowledged.

**Conflicts of Interest:** The authors declare no conflicts of interest.

## References

1. Hartog, A.H. *An Introduction to Distributed Optical Fibre Sensors*; CRC Press: Boca Raton, FL, USA, 2017. [CrossRef]
2. Gorshkov, B.G.; Yüksel, K.; Fotiadi, A.A.; Wuilpart, M.; Korobko, D.A.; Zhirnov, A.A.; Stepanov, K.V.; Turov, A.T.; Konstantinov, Y.A.; Lobach, I.A. Scientific Applications of Distributed Acoustic Sensing: State-of-the-Art Review and Perspective. *Sensors* **2022**, *22*, 1033. [CrossRef] [PubMed]
3. Zhang, S.; Xie, S.; Li, Y.; Yuan, M.; Qian, X. Detection of Gas Pipeline Leakage Using Distributed Optical Fiber Sensors: Multi-Physics Analysis of Leakage-Fiber Coupling Mechanism in Soil Environment. *Sensors* **2023**, *23*, 5430. [CrossRef] [PubMed]
4. Gietz, H.; Sharma, J.; Tyagi, M. Machine Learning for Automated Sand Transport Monitoring in a Pipeline Using Distributed Acoustic Sensor Data. *IEEE Sensors J.* **2024**, *24*, 22444–22457. [CrossRef]
5. Ghazali, M.F.; Mohamad, H.; Nasir, M.Y.M.; Hamzh, A.; Abdullah, M.A.; Aziz, N.F.A.; Thansirichaisree, P.; Zan, M.S.D. State-of-The-Art application and challenges of optical fibre distributed acoustic sensing in civil engineering. *Opt. Fiber Technol.* **2024**, *87*, 103911. [CrossRef]
6. Dejdar, P.; Záviška, P.; Valach, S.; Münster, P.; Horváth, T. Image Edge Detection Methods in Perimeter Security Systems Using Distributed Fiber Optical Sensing. *Sensors* **2022**, *22*, 4573. [CrossRef]
7. Gao, Y.; Cai, Q. Application of Smart Fiber Optic Sensor Technology in Feature Extraction, Recognition, and Detection. *Wirel. Commun. Mob. Comput.* **2022**, *2022*, 4552388. [CrossRef]
8. Fernandez-Ruiz, M.R.; Martins, H.F.; Williams, E.F.; Becerril, C.; Magalhaes, R.; Costa, L.; Martin-Lopez, S.; Jia, Z.; Zhan, Z.; Gonzalez-Herraez, M. Seismic Monitoring With Distributed Acoustic Sensing From the Near-Surface to the Deep Oceans. *J. Light. Technol.* **2022**, *40*, 1453–1463. [CrossRef]
9. Jousset, P.; Reinsch, T.; Ryberg, T.; Blanck, H.; Clarke, A.; Aghayev, R.; Hersir, G.P.; Henninges, J.; Weber, M.; Krawczyk, C.M. Dynamic strain determination using fibre-optic cables allows imaging of seismological and structural features. *Nat. Commun.* **2018**, *9*, 2509. [CrossRef]
10. Yin, J.; Zhu, W.; Li, J.; Biondi, E.; Miao, Y.; Spica, Z.J.; Viens, L.; Shinohara, M.; Ide, S.; Mochizuki, K.; et al. Earthquake Magnitude With DAS: A Transferable Data-Based Scaling Relation. *Geophys. Res. Lett.* **2023**, *50*, e2023GL103045. [CrossRef]
11. Miao, Y.; Salaree, A.; Spica, Z.J.; Nishida, K.; Yamada, T.; Shinohara, M. Assessing the Earthquake Recording Capability of an Ocean-Bottom Distributed Acoustic Sensing Array in the Sanriku Region, Japan. *Seismol. Res. Lett.* **2025**, *96*, 631–650. . [CrossRef]
12. Gök, R.; Walter, W.R.; Barno, J.; Downie, C.; Mellors, R.J.; Mayeda, K.; Roman-Nieves, J.; Templeton, D.; Ajo-Franklin, J. Reliable Earthquake Source Parameters Using Distributed Acoustic Sensing Data Derived from Coda Envelopes. *Seismol. Res. Lett.* **2024**, *95*, 2208–2220. [CrossRef]
13. Lior, I.; Rivet, D.; Ampuero, J.P.; Sladen, A.; Barrientos, S.; Sánchez-Olavarría, R.; Villarroel Opazo, G.A.; Bustamante Prado, J.A. Magnitude estimation and ground motion prediction to harness fiber optic distributed acoustic sensing for earthquake early warning. *Sci. Rep.* **2023**, *13*, 424. [CrossRef]
14. Carlino, S.; Mirabile, M.; Troise, C.; Sacchi, M.; Zeni, L.; Minardo, A.; Caccavale, M.; Darányi, V.; De Natale, G. Distributed-Temperature-Sensing Using Optical Methods: A First Application in the Offshore Area of Campi Flegrei Caldera (Southern Italy) for Volcano Monitoring. *Remote Sens.* **2016**, *8*, 674. [CrossRef]
15. Wilcock, W.S.; Abadi, S.; Lipovsky, B.P. Distributed acoustic sensing recordings of low-frequency whale calls and ship noise offshore Central Oregon. *JASA Express Lett.* **2023**, *3*, 026002. [CrossRef] [PubMed]
16. Rivet, D.; de Cacqueray, B.; Sladen, A.; Roques, A.; Calbris, G. Preliminary assessment of ship detection and trajectory evaluation using distributed acoustic sensing on an optical fiber telecom cable. *J. Acoust. Soc. Am.* **2021**, *149*, 2615–2627. [CrossRef]
17. Xiao, H.; Spica, Z.J.; Li, J.; Zhan, Z. Detection of Earthquake Infragravity and Tsunami Waves With Underwater Distributed Acoustic Sensing. *Geophys. Res. Lett.* **2024**, *51*, e2023GL106767. [CrossRef]
18. Landrø, M.; Bouffaut, L.; Kriesell, H.J.; Potter, J.R.; Rørstadbotnen, R.A.; Taweesintananon, K.; Johansen, S.E.; Brenne, J.K.; Haukanes, A.; Schjelderup, O.; et al. Sensing whales, storms, ships and earthquakes using an Arctic fibre optic cable. *Sci. Rep.* **2022**, *12*, 19226. [CrossRef]
19. Lior, I.; Sladen, A.; Rivet, D.; Ampuero, J.P.; Hello, Y.; Becerril, C.; Martins, H.F.; Lamare, P.; Jestin, C.; Tsagkli, S.; et al. On the detection capabilities of underwater distributed acoustic sensing. *J. Geophys. Res. Solid Earth* **2021**, *126*, e2020JB020925. [CrossRef]
20. Sladen, A.; Rivet, D.; Ampuero, J.P.; De Barros, L.; Hello, Y.; Calbris, G.; Lamare, P. Distributed sensing of earthquakes and ocean-solid Earth interactions on seafloor telecom cables. *Nat. Commun.* **2019**, *10*, 5777. [CrossRef]

21. Howe, B.M.; Angove, M.; Aucan, J.; Barnes, C.R.; Barros, J.S.; Bayliff, N.; Becker, N.C.; Carrilho, F.; Fouch, M.J.; Fry, B.; et al. SMART Subsea Cables for Observing the Earth and Ocean, Mitigating Environmental Hazards, and Supporting the Blue Economy. *Front. Earth Sci.* **2022**, *9*, 775544. [CrossRef]
22. Favali, P.; Beranzoli, L.; D'Anna, G.; Gasparoni, F.; Gerber, H.W. NEMO-SN-1 the first "real-time" seafloor observatory of ESONET. *Nucl. Instruments Methods Phys. Res. Sect. A Accel. Spectrometers Detect. Assoc. Equip.* **2006**, *567*, 462–467. [CrossRef]
23. Pulvirenti, S.; Viola, S. The INFN-LNS Fibre optic infrastructure. In Proceedings of the Galileo Conference: Fibre Optic Sensing in Geosciences, Catania, Italy, 16–20 June 2024. . [CrossRef]
24. Azzaro, R. Earthquake surface faulting at Mount Etna volcano (Sicily) and implications for active tectonics. *J. Geodyn.* **1999**, *28*, 193–213. [CrossRef]
25. Gutscher, M.A.; Quetel, L.; Murphy, S.; Riccobene, G.; Royer, J.Y.; Barreca, G.; Aurnia, S.; Klingelhoefer, F.; Cappelli, G.; Urlaub, M.; et al. Detecting strain with a fiber optic cable on the seafloor offshore Mount Etna, Southern Italy. *Earth Planet. Sci. Lett.* **2023**, *616*, 118230. [CrossRef]
26. Viola, S.; Grammauta, R.; Sciacca, V.; Bellia, G.; Beranzoli, L.; Buscaino, G.; Caruso, F.; Chierici, F.; Cuttone, G.; D'Amico, A.; et al. Continuous monitoring of noise levels in the Gulf of Catania (Ionian Sea). Study of correlation with ship traffic. *Mar. Pollut. Bull.* **2017**, *121*, 97–103. [CrossRef]
27. Sciacca, V.; Caruso, F.; Beranzoli, L.; Chierici, F.; De Domenico, E.; Embriaco, D.; Favali, P.; Giovanetti, G.; Larosa, G.; Marinaro, G.; et al. Annual Acoustic Presence of Fin Whale (Balaenoptera physalus) Offshore Eastern Sicily, Central Mediterranean Sea. *PLoS ONE* **2015**, *10*, e0141838. [CrossRef]
28. Caruso, F.; Alonge, G.; Bellia, G.; De Domenico, E.; Grammauta, R.; Larosa, G.; Mazzola, S.; Riccobene, G.; Pavan, G.; Papale, E.; et al. Long-term monitoring of dolphin biosonar activity in deep pelagic waters of the Mediterranean Sea. *Sci. Rep.* **2017**, *7*, 4321. [CrossRef]
29. Favali, P.; Chierici, F.; Marinaro, G.; Giovanetti, G.; Azzarone, A.; Beranzoli, L.; De Santis, A.; Embriaco, D.; Monna, S.; Lo Bue, N.; et al. NEMO-SN1 Abyssal Cabled Observatory in the Western Ionian Sea. *IEEE J. Ocean. Eng.* **2013**, *38*, 358–374. [CrossRef]
30. Di Mauro, L.S.; Diego-Tortosa, D.; Riccobene, G.; D'Amato, C.; Leonora, E.; Longhitano, F.; Orlando, A.; Viola, S. The IPANEMA Project: Underwater Acoustic Structure for Volcanic Activity and Natural CO2 Emissions Monitoring. *Eng. Proc.* **2023**, *58*, 9. [CrossRef]
31. Gutscher, M.A.; Royer, J.Y.; Graindorge, D.; Murphy, S.; Klingelhoefer, F.; Aiken, C.; Cattaneo, A.; Barreca, G.; Quetel, L.; Riccobene, G.; et al. Fiber optic monitoring of active faults at the seafloor: I the FOCUS project. *Photoniques* **2019**, 32–37.
32. Dean, T.; Cuny, T.; Hartog, A.H. The effect of gauge length on axially incident P-waves measured using fibre optic distributed vibration sensing. *Geophys. Prospect.* **2017**, *65*, 184–193. [CrossRef]
33. Hubbard, P.G.; Vantassel, J.P.; Cox, B.R.; Rector, J.W.; Yust, M.B.S.; Soga, K. Quantifying the Surface Strain Field Induced by Active Sources with Distributed Acoustic Sensing: Theory and Practice. *Sensors* **2022**, *22*, 4589. [CrossRef] [PubMed]
34. Istituto Nazionale di Geofisica e Vulcanologia (INGV). Earthquake Report: Event ID 36866661. *INGV Terremoti* **2023**. Available online: https://terremoti.ingv.it/en/event/36866661 (accessed on 24 March 2025).
35. Calò, M.; Parisi, L.; Luzio, D. Lithospheric P- and S-wave velocity models of the Sicilian area using WAM tomography: Procedure and assessments. *Geophys. J. Int.* **2013**, *195*, 625–649. [CrossRef]
36. Diego-Tortosa, D.; Bonanno, D.; Bou-Cabo, M.; Di Mauro, L.S.; Idrissi, A.; Lara, G.; Riccobene, G.; Sanfilippo, S.; Viola, S. Effective Strategies for Automatic Analysis of Acoustic Signals in Long-Term Monitoring. *J. Mar. Sci. Eng.* **2025**, *13*, 454. [CrossRef]
37. Celli, N.L.; Bean, C.J.; O'Brien, G.S. Full-waveform simulation of DAS records, response and cable-ground coupling. *Geophys. J. Int.* **2023**, *236*, 659–674. [CrossRef]
38. Williams, E.F.; Fernández-Ruiz, M.R.; Magalhaes, R.; Vanthillo, R.; Zhan, Z.; González-Herráez, M.; Martins, H.F. Distributed sensing of microseisms and teleseisms with submarine dark fibers. *Nat. Commun.* **2019**, *10*, 5778. [CrossRef]
39. McKenna, M.F.; Ross, D.; Wiggins, S.M.; Hildebrand, J.A. Underwater radiated noise from modern commercial ships. *J. Acoust. Soc. Am.* **2012**, *131*, 92–103 . [CrossRef]
40. Traverso, F.; Gaggero, T.; Rizzuto, E.; Trucco, A. Spectral analysis of the underwater acoustic noise radiated by ships with controllable pitch propellers. In Proceedings of the OCEANS 2015, Genova, Italy, 18–21 May 2015; pp. 1–6. [CrossRef]
41. Dekeling, R.; Tasker, M.; Van der Graaf, S.; Ainslie, M.; Andersson, M.; André, M.; Borsani, J.; Brensing, K.; Castellote, M.; Cronin, D.; et al. *Monitoring Guidance for Underwater Noise in European Seas—Part I: Executive Summary*; Number JRC88733 in EUR 26557; Publications Office of the European Union: Luxembourg, 2014. [CrossRef]
42. Dekeling, R.; Tasker, M.; Van der Graaf, S.; Ainslie, M.; Andersson, M.; André, M.; Borsani, J.; Brensing, K.; Castellote, M.; Cronin, D.; et al. *Monitoring Guidance for Underwater Noise in European Seas—Part II: Monitoring Guidance Specifications*; Number JRC88045 in EUR 26555; Publications Office of the European Union: Luxembourg, 2014. [CrossRef]

43. Halliday, W.D.; Insley, S.J.; Hilliard, R.C.; de Jong, T.; Pine, M.K. Potential impacts of shipping noise on marine mammals in the western Canadian Arctic. *Mar. Pollut. Bull.* **2017**, *123*, 73–82. [CrossRef]
44. Matsumoto, H.; Araki, E.; Kimura, T.; Fujie, G.; Shiraishi, K.; Tonegawa, T.; Obana, K.; Arai, R.; Kaiho, Y.; Nakamura, Y.; et al. Detection of hydroacoustic signals on a fiber-optic submarine cable. *Sci. Rep.* **2021**, *11*, 2797. [CrossRef]